Preprints (www.preprints.org) | NOT PEER-REVIEWED | Posted: 26 July 2017 doi:10.20944/preprints201707.0076.v1

Review

Ultraviolet imaging of volcanic plumes: a new paradigm in volcanology

Andrew J.S. McGonigle [1,2,3,*], Tom D. Pering [1], Thomas C. Wilkes [1], Giancarlo Tamburello [4], Roberto D'Aleo [5], Marcello Bitetto [5], Alessandro Aiuppa [2,5]

1 Department of Geography, University of Sheffield, Sheffield, S10 2TN, UK; t.pering@sheffield.ac.uk (T.D.P.); tcwilkes@sheffield.ac.uk (T.C.W.).
2 Istituto Nazionale di Geofisica e Vulcanologia, Sezione di Palermo, Via Ugo La Malfa 153, 90146 Palermo, Italy.
3 School of Geosciences, The University of Sydney, Sydney, NSW 2006, Australia
4 Istituto Nazionale di Geofisica e Vulcanologia, Sezione di Bologna, Via Donato Creti, 12, 40100 Bologna, Italy; giancarlo.tamburello@ingv.it (G.T.).
5 DiSTeM, Università di Palermo, via Archirafi, 22, 90123 Palermo, Italy; roberto.daleo01@unipa.it (R.D.); marcellobitetto@gmail.com (M.B.); aiuppa@unipa.it (A.A.).

* Correspondence: a.mcgonigle@sheffield.ac.uk; Tel.: +44-114-222-7961

Abstract: Ultraviolet imaging has been applied in volcanology over the last ten years or so. This provides considerably higher temporal and spatial resolution volcanic gas emission rate data than available previously, enabling the volcanology community to investigate a range of far faster plume degassing processes, than achievable hitherto. To date this has covered rapid oscillations in passive degassing through conduits and lava lakes, as well as puffing and explosions, facilitating exciting connections to be made for the first time between previously rather separate sub disciplines of volcanology. Firstly, there has been corroboration between geophysical and degassing datasets at ≈ 1 Hz expediting more holistic investigations of volcanic source-process behaviour. Secondly, there has been the combination of surface observations of gas release, with fluid dynamic models (numerical, mathematical and laboratory) for gas flow in conduits, in attempts to link subterranean driving flow processes to surface activity types. There has also been considerable research and development concerning the technique itself, covering error analysis and most recently adaptation of smartphone sensors for this application, to deliver gas fluxes at a significantly lower instrumental price point than possible previously. At this decadal juncture in the application of UV imaging in volcanology, this article provides an overview of what has been achieved to date as well as a forward look to potential future research directions, in particular covering the first use of UV cameras to generate volcanic gas composition ratio imagery.

Keywords: ultraviolet cameras; volcanic plumes; interdisciplinary volcanology

1. Introduction

Volcanoes are observed in two primary ways: firstly by measurements of geophysical signatures e.g., seismic, thermal and acoustic; and secondly, through observations of gases released from summit craters, flanks or fumaroles [1]. Historically, the degassing data have been considered as somewhat secondary to those from geophysics, in particularly seismic data, largely because of limitations in the applied instrumentation. However, during the last two decades there has been a major renaissance in volcanic gas monitoring, arising from the implementation of exciting new ground based technologies for measuring the gases released in volcanic plumes. These approaches have been of utility in increasing our understanding of the underground processes, which drive surface activity, as well as in routine volcano monitoring operations.

© 2017 by the author(s). Distributed under a Creative Commons CC BY license.

Preprints (www.preprints.org) | NOT PEER-REVIEWED | Posted: 26 July 2017 doi:10.20944/preprints201707.0076.v1

These recently applied techniques fall into two categories: firstly those that concern the chemical composition of the gases, e.g., Fourier Transform Infrared spectroscopy [2] and MultiGAS units [3], and secondly those that capture emission rates or fluxes. The latter data have been largely focused on sulphur dioxide (SO_2), which is straightforward to remotely sense in volcanic plumes due to its strong ultraviolet (UV) absorption bands, and low ambient concentrations. There have also been exciting recent developments concerning LIDAR remote sensing of carbon dioxide (CO_2) emissions, e.g., [4; this volume] from volcanoes.

UV remote sensing of SO_2 emissions has been conducted since the 1970s, initially with correlation spectrometer (COSPEC) units developed for monitoring smokestack emissions from coal burning power stations, leading to generation of a number of valuable long-term datasets [5,6]. Since the turn of the century, these units have been replaced with low cost USB coupled linear array spectrometers, costing only a few thousand dollars, an order of magnitude less than COSPEC [7,8]. Data analysis to deliver SO_2 column amounts is achieved using differential optical absorption spectroscopy routines, and the units have been applied from mobile units, e.g., on cars and aeroplanes, whilst traversing beneath a plume, as well as in fixed position deployments, involving scanning optics [9,10]. These scanning spectrometers are now in routine operation on numerous volcanoes, worldwide [11,12].

Notwithstanding the benefits of the above technology, and its service within the volcanology community, the acquired data are limited in time resolution to a datum every 100s or so, due to the requirement to physically scan or traverse the plume. This is too slow to resolve many rapid gas driven volcanic processes, e.g., puffing and strombolian explosions, such that the acquired data cannot be used to investigate the driving underground fluid dynamics in these cases. Indeed, the only way to scrutinise these more rapid phenomena, was via geophysical data, which are acquired at frequencies of at least 1 Hz, leading to somewhat indirect proxy understanding. This prompted several research groups [e.g., 13,14] to pioneer UV imaging approaches, which provide image snapshots of the plume gas concentrations every second or so, from which gas fluxes can be generated at the same time resolution. In this article, we cover technological aspects of the application of UV imagery within volcanology, followed by an overview of the present and potential future scientific possibilities that this approach brings to the field.

2. Ultraviolet camera instrumentation

The UV cameras operation is based on imaging gas plumes, which arise from the summit craters of volcanoes or fumarole fields, with a bandpass filter mounted to the fore of the unit, centered around 310 nm, where SO_2 absorbs incident radiation. Typically, imagery at 330 nm is also acquired, where there is no SO_2 absorption, to factor out broadband aerosol related issues, which are common to both wavebands. This can be achieved using two co-aligned cameras, or a single camera, and a filter wheel. Below is a brief overview of the measurement approach, which is detailed further in Kantzas et al. [15], for the more robust two camera, two filter setup.

Firstly, optimal exposure settings are determined for each camera, based on the skylight illumination intensity, to maximize signal-to-noise and avoid saturation whilst viewing the sky. The next step is to measure dark images, at these exposure times, in order to account for the camera response, when light is blocked from entering the fore-optics. Following this, background sky images are acquired for each camera, by imaging a region of sky, adjacent to the plume, e.g., containing no gas absorption. At this stage, the cameras are pointed at the plume and the measurement sequence begins. Following Beer's law these images are processed to provide uncalibrated apparent absorption, AA for each pixel via the following relationship:

$$AA = -\log_{10}\left[\frac{IP_{310} - ID_{310}}{IB_{310} - ID_{310}} \Big/ \frac{IP_{330} - ID_{330}}{IB_{330} - ID_{330}}\right] \quad (1)$$

Preprints (www.preprints.org) | NOT PEER-REVIEWED | Posted: 26 July 2017 doi:10.20944/preprints201707.0076.v1

Here, *IP* is the intensity, whilst viewing the plume, *IB* is the background sky intensity and *ID* is the dark intensity for the pixel in question, where the subscripts pertain to the camera filter wavelength. Following determination of apparent absorption images, calibration is required. This can be achieved with quartz cells containing known column amounts of SO_2. In this case, *AA* values are determined for each cell, and averaged over a section in the centre of the image. These data are plotted on a scatter plot of axes: cell column amount vs. apparent absorption. The gradient of the best-fit line is then extracted, acting as the calibration factor, which all volcanic plume image pixel *AA* values are then multiplied by. An alternative approach to calibration is to use a co-aligned spectrometer to determine a column amount value corresponding to a small section of the image, to enable scaling to calibrated concentration values across the whole image. Once calibrated images are generated, a cross section line through the plume is defined and all column amounts are integrated along this to determine the so-called total column amount. Plume speed is then found, often by determining integrated column amount time series, from cross sections drawn through the plume at two different distances above the crater. These series are then cross-correlated to determine the temporal lag between them, from which transit speed can be found [16,17]. Alternately, motion-tracking algorithms have been applied to find plume velocities [18]. Multiplication of the transport speed by one of the integrated column amount time series leads to generation of flux time series.

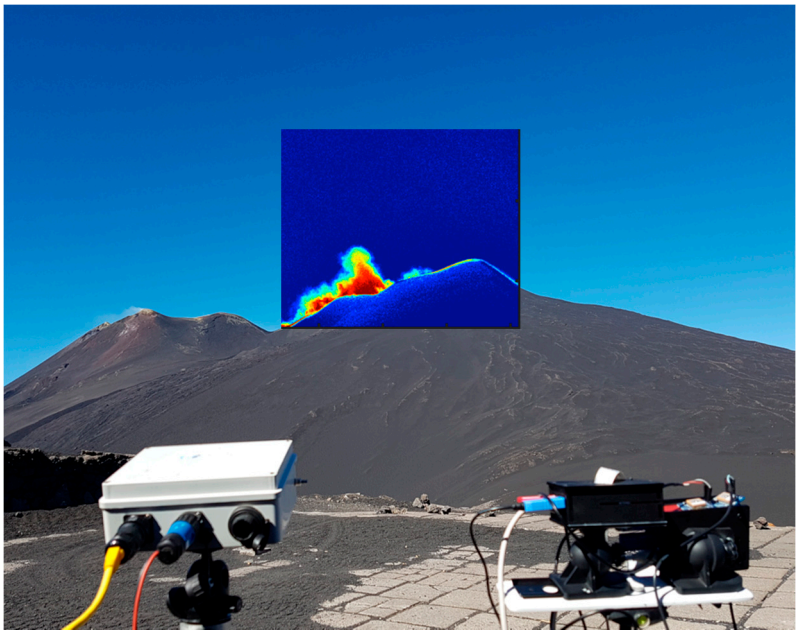

Figure 1. Deployment of inexpensive smartphone sensor based UV camera instrumentation (right) in tandem with more traditionally applied scientific grade cameras (left) on Mt. Etna. Inset shows false colouration of SO_2 concentrations from the cheaper units, which were based on modified Raspberry Pi cameras. For further detail see [19] and [20].

Errors in flux computations are thought to be in the region of 20-30% [21]. Errors arise from scattering of radiation between the sensor and the plume, e.g., light dilution as well as scattering within the plume itself [22,23]. There are also uncertainties arising from cell calibration [24], as well as from light transit through the filters at different incident angles [25]. One approach that could mitigate against radiative transfer related errors is a Fabry-Perot configuration [26, 27]. To date most of the camera systems applied in this context have been based on commercially available UV cameras, with price points of thousands of USD. Recently, however, low-cost sensors, designed primarily for the smartphone market have been adapted for this application, such that usable UV sensitivity of these units has been demonstrated [19], as well as signal-to-noise characteristics, which are not dissimilar to those of the more expensive, traditionally applied units [20] (Figure 1).

Preprints (www.preprints.org) | NOT PEER-REVIEWED | Posted: 26 July 2017 doi:10.20944/preprints201707.0076.v1

3. Improving spatio-temporal resolution of volcanic degassing

The cameras have now been deployed on a significant number of volcanoes worldwide, due in part to the convenience of being able to set up and operate from fixed positions during discrete field campaigns [e.g., 28,29]. To date, the targets covered by permanent network installations have been rather fewer, e.g., Etna, Stromboli and Kīlauea [30-34], potentially as a consequence of the large cost of the scientific grade cameras, typically used in these deployments, as well as the requirement to image the plume, e.g., without cloud cover between the camera and summit area. There is, of course, meteorological cloud cover at the top of volcanoes, which can occlude observations. Herein lies one advantage of conventional spectroscopic gas flux assessments, in that imaging is not a requirement for this class of observation.

The cameras provide the possibility of resolving spatio-temporal degassing characteristics in unprecedented details. For instance, spatial information was typically only available hitherto from volcanoes with multiple craters, by the rare occurrence of walking traverse observations made very close to source [35]. By gathering spatial information, the cameras implicitly provide scope for resolution of gas fluxes from heterogenous sources, as exploited on Vulcano island, to measure gas fluxes from individual fumaroles [36]. This capability has also been exploited in respect of multiple crater scenarios, e.g., Mt. Etna, where shifting of degassing from one vent to another has been observed in tandem with transference of eruptive activity between these sources [31].

In terms of temporal information, the UV cameras have enabled us to capture rapid trends in passive and explosive degassing. In particular, fluctuations in passive degassing on timescales of 10s to 1000s of seconds have been resolved using UV cameras [37], building on earlier observations of this phenomenon using a non-imaging dual spectrometer approach, involving units with cylindrical lenses and quasi-horizontal fields of view [38,39]. Based on observations on Mt. Etna, Mayon and Erebus, using contemporaneous Multi-GAS observations and/or ancillary visible/near IR cameras, these fluctuations appear to also be manifested in degassing of CO_2 and water vapour emissions [40-42]. This behaviour has been observed in both conduit degassing scenarios (e.g., Mt Etna) as well as from lava lakes. In terms of conduit degassing, arguments have been put forward that this behaviour arises from arrangement of rising bubbles into layers of elevated gas concentrations, leading to periodic enhancements in passive non-overpressurised bubble bursting at the surface [37].

The situation with lava lakes is intriguing in that rather different degassing trends have been observed from each of the volcanoes targeted to date with high time resolution gas flux observations, e.g., Villarrica, Chile [43], Kīlauea, Hawaii [44] and Erebus, Antarctica [39]. This potentially points to a wide variety of gas flow processes occurring across these systems, which range significantly, both in magmatic viscosities as well as in gas flux magnitudes. In particular, 'gas pistoning' is evident in the Kīlauea data, involving pronounced spikes in degassing, followed by a gradual waning in emissions, on timescales of tens of minutes, potentially caused by a gas accumulation and release mechanism. In contrast, Erebus volcano demonstrates stable periodic degassing behaviour, present in both the acquired gas flux and gas composition time series [39], thought to arise from a stable bi-directional flow in the conduit, such that gas rich magma batches periodically rise, degas then sink down again into the conduit. In Villarrica, gas flux time series data revealed no stable periodicity in degassing. This is thought to be precluded by turbulent mixing in the lava lake, arising from continuous inflow of magma from the conduit [43].

One major application of the UV cameras has been to measure gas masses released during discrete explosions. Whilst this has been achieved spectroscopically with high temporal resolution differential optical absorption spectroscopy observations [38], and even with a correlation spectrometer [45], it is far easier to resolve these emissions with the cameras' imaging capacity. The eruptions where SO_2 masses have been constrained with UV imagery have been ash-poor, strombolian, or weakly vulcanian events. Whilst UV imaging of ash rich plumes has been acheived, yielding interesting insights into the ash phase plume dynamics [46], the reduction in optical thickness caused by ash in these cases, rules out retrieval of SO_2 emissions. Interestingly, these explosive UV camera studies typically point towards non-explosive release of gas as being the

Preprints (www.preprints.org) | NOT PEER-REVIEWED | Posted: 26 July 2017 doi:10.20944/preprints201707.0076.v1

dominant means by which these volcanoes release volatiles to the atmosphere [21,47-52], especially for basaltic open conduit cases, such as Etna and Stromboli, where gas bubbles are free to move through the melt. In particular, Tamburello et al. [47] reported that, for Stromboli volcano, degassing was partitioned as 77% passive gas release (e.g., from spherical bubbles), 16% from puffing, e.g., from cap bubbles and with only 7% from explosions, e.g., from gas slugs (Taylor bubbles). This study, incidentally, also constituted the first direct measurement of puffing gas masses on a volcano, pointing to the real benefits of the camera technology in terms of its high spatial resolution and sufficiently good sensitivity to capture these subtle degassing features.

In these reports, the subdivision of fluxing between the degassing classes appears to be most strongly tipped towards explosive release (although is still often dominated by passive degassing) in the scenarios where eruptions are more vulcanian in nature [21, 50-52], e.g., Santiaguito, Asama, Semeru and Fuego volcanoes. In particular, Smekens et al. [50], suggest, in respect of the Semeru observations, that accumulation and pressurisation beneath a viscous plug are in operation, before breach and explosive release. This assertion is intuitive and follows on from that put forth following pioneering observations on Karymsky volcano by Fischer et al. [44], where dominantly explosive gas release was reported, based on correlation spectrometer observations made long before the advent of UV imaging.

4. Combination of UV camera degassing data with geophysical data and conduit fluid dynamics

The above studies point to the absolute necessity of models to facilitate interpretation of the acquired data. In this respect, the high time resolution of the UV cameras has an enormous benefit for volcanology. Specifically, the cameras can resolve gas release processes, which are caused by a variety of subterranean fluid dynamic mechanisms, which have been the subject of considerable prior numerical, mathematical and laboratory modeling efforts, both within the volcanic and engineering research communities. This is especially so in the case of strombolian explosions, which are thought to arise from bursting of conduit filling gas slugs at the surface [53]. Here, in one of the most exciting current frontiers in volcanology, UV camera data are enabling the first substantive bridging between the volcanic gas measurement and volcanic conduit fluid dynamic modeling communities.

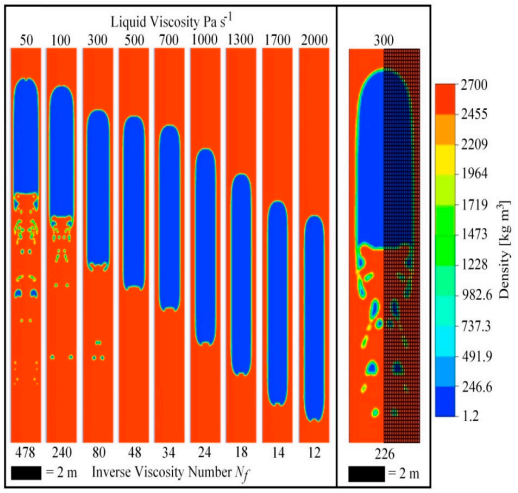

Figure 2. Computational fluid dynamic modeling of rising gas slugs on Stromboli, illustrating fissuring of daughter bubbles from the slug base. This has been linked to codas in UV camera gas flux time series following strombolian explosions, illustrating the potential of combining models with high time resolution field degassing data to unravel the subterranean drivers of surface activity. See main text and [33] for more detail.

In particular, Pering et al. [33] have studied explosions on Stromboli, where a tail or coda in emissions was observed following the events. They interpreted the activity, with the aid of computational fluid dynamic models, as arising from the fissioning of smaller "daughter" bubbles from the bases of the rising slugs (Fig. 2). Furthermore, during a study of rapid (0.25 Hz) strombolian

Preprints (www.preprints.org) | NOT PEER-REVIEWED | Posted: 26 July 2017 doi:10.20944/preprints201707.0076.v1

activity on Mt. Etna, explosive data were plotted on a scatter plot of repose time following the event vs. event mass [49]. An absence of large mass, long repose time data were noted, which was interpreted as being due to coalescence of adjacent rising slugs, e.g., leading to a longer repose interval before the arrival of the next distinct slug, and constituting the first direct empirical evidence of slug interaction in volcanic conduits. A follow on report, based on thermal observations of puffing on Stromboli, also affirms the potential importance of this process in respect of cap bubbles [54].

Another important benefit of the UV camera data, is that the high time resolution gas fluxes can be compared with contemporaneous geophysical data, with far less aliasing than necessary previously e.g., the latter data are acquired at frequencies ≥ 1 Hz. This is highly significant in that many geophysical manifestations on volcanoes arise from gas based processes, e.g., seismic signals caused by the ascent of gas slugs in conduits, and thermal and infrasonic signatures generated from the surficial bursting of these bubbles. Until now we have had to rely purely on geophysical means to understand rapid degassing processes on volcanoes, e.g., strombolian explosions and puffing. Not only do the UV camera data provide a more direct means of understanding these phenomena, but they also enable the possibility of making far more direct comparison with geophysical series, which could lead the way towards better interpretation of geophysical observations on volcanoes and more holistic understanding of volcanic behaviour.

The first report of high time resolution (≈ 1 Hz) degassing data being corroborated with geophysical data concerned explosions on Stromboli volcano [38]. This study was performed using spectroscopy, rather than UV imaging, but, in common with a more recent UV camera study on this target [47], it revealed linear correlations between the magnitudes of the recorded degassing, thermal and very long period (VLP) seismic signatures for the events. This fits with the conventionally held, although previously rather hypothetical, view that VLP signals on Stromboli arise from volumetric changes associated with the ascent of gas masses e.g., slugs in the conduit, such that the larger the rising gas mass, the greater the VLP signal. Further related investigations have been performed on Asama [51] and Fuego [52] volcanoes, where proportionality between VLP signals and released SO_2 masses, was also observed. The relative scaling of seismic moment with released SO_2 mass does seem to be rather larger for Asama, than for the other targets, which may be related to an absence of gas ratio information, e.g., total released gas masses are not being considered. However, it is also highly likely that volcano specific features, e.g., the conduit geometry, magma rheology and the precise mechanism of VLP generation, which is likely to vary between the targets, will affect the degree to which the degassing processes are coupled into seismic energy in each case.

Ultraviolet imaging degassing fluxes have also been linked to tremor, a class of seismicity associated with pressure fluctuations in degassing magmas. Here a number of studies have noted a relationship between these time series for Etna, Fuego, and Kilauea volcanoes, including conduit and lava lake degassing scenarios [37, 42, 44, 55]. In one case, this has involved a novel signal processing techniques, based on wavelet analysis to isolate commonality in periodicity in pairs of geophysical datastreams [56]. These experimental outcomes are as would be expected, given that tremor is anticipated to increase with elevated bubble concentrations in magmas, or more rapid flow of bubbles in the conduit, scenarios which would both correspond to periods of elevated gas release. In two of the studies, intriguing lag relationships were identified [42, 55]. In particular, in Nadeau et al. [55] a trend of increasing temporal lags between the seismic and gas flux time series was observed, in the period following explosions, implying, perhaps that the source of seismic energy was becoming progressively deeper within the conduit, due to rheological stiffening of the magma, downwards from the top of the column. In Pering et al. [42] bursts in CO_2 outgassing were reported (derived from the UV cameras in tandem with Multi-GAS [3] units) which preceded spikes in seismicity, raising intriguing questions regarding the causal processes, which might link these phenomena in this case.

Thermal observations have also been correlated with UV camera data, with the most detailed study to date in this area being that of Tamburello et al. [47] concerning explosions on Stromboli,

Preprints (www.preprints.org) | NOT PEER-REVIEWED | Posted: 26 July 2017 doi:10.20944/preprints201707.0076.v1

building on an earlier more limited treatment on this target [38]. Both resulting articles demonstrated a linear relationship between these two parameters, although in the more recent one, two populations arose, corresponding to events, which were ash free/with ash, respectively. This is as would be expected, e.g., the ashier eruptions will be thermally brighter due to the larger quantity of radiating solid ejecta. In addition, UV camera/high time resolution spectroscopic instrumentation based attempts have been made to compare SO_2 fluxes with acoustic data in respect of explosive activity, resulting in reports of either no [38] or somewhat limited [57] correlations being apparent between these time series. A significant breakthrough in this regard has come with the application of linear acoustic processing of the acquired infrasonic signals to infer gas masses. This methodology, which involves consideration of the entire waveform, and not merely initial pressure conditions, led to 1:1 linear correlations with contemporaneously acquired UV camera derived gas masses [32].

5. Future directions

Ultraviolet camera technology provides an unprecedented opportunity to investigate volcanic degassing behaviour with far better spatial and temporal resolution than possible previously. This has expedited linkage of gas fluxes with geophysical data and conduit fluid dynamic models in ways that were impossible hitherto, opening the path to a number of potentially very fruitful future research directions.

In particular, the comparison of high time resolution UV camera gas fluxes with modeled emission rates from laboratory and computational fluid dynamics is an area of study in its absolute infancy. By simulating degassing behaviour from a series of underground gas flow mechanisms, and comparing against field data to determine best matches e.g., using correlative approaches, new avenues will be opened in terms of being able to understand how subterranean processes drive volcanism. We recently combined these approaches for the first time [33], illustrating the exciting scientific potential contained therein, in a study of strombolian activity on Strombolian volcano. There is now much work remaining to be done, in expanding this methodology to unravel degassing dynamics across a wide spectrum of activity styles and volcanic targets. This will encourage further developments in the models themselves, which have been somewhat focused on slug dynamics to date [e.g., 53], to give greater attention to other potential fluid processes in volcanoes e.g., bubbly, cap, annular and churn flow mechanisms.

The linking of UV camera degassing data to geophysical data on timescales of ≈1 Hz has led to the establishments of correlations between degassing data and volcano-seismic and acoustic signals. This could enable calibration of acquired acoustic and seismic signals to infer gas masses, thereby helping to overcome one the key limitations of the UV camera approach, namely inoperability at night-time and when the plume cannot be imaged, due to cloud cover [32, 51]. Hence, whilst the UV cameras deliver the most direct estimates of the degassing output from volcanoes, these calibrated geophysical proxies could be used to straddle windows where the cameras cannot be used, enabling continuous monitoring to take place. Another dimension of corroboration between the geophysical and UV camera degassing signals will be to better understand how underground degassing processes are responsible for generating geophysical manifestations on volcanoes. A key aim here would be to attempt to identify ≈1 Hz multi-parametric (e.g., geophysical and degassing) signatures, which precede eruptions, to establish precursory templates. This will build on pioneering studies, which have already illustrated the profound scientific insights achievable by blending these disparate data, albeit on the basis of previously available coarse time resolution gas flux data [e.g., 58]. This linkage of ground based gas fluxes, models and geophysical data, will also mirror similar integrated initiatives to combine these approaches on the basis of satellite observations, which are enabling significant breakthroughs in volcanology [59].

There is much that remains to be achieved in the UV camera hardware too. To date the uptake of these cameras in routine monitoring has been somewhat limited, in part perhaps due to the relatively high cost of the commercially available units (thousands of USD) typically used in this application area. However, the recent proof of concept demonstration, that order of magnitude cheaper smartphone sensor based systems can be used in volcanic SO_2 monitoring [19,20] may

Preprints (www.preprints.org) | NOT PEER-REVIEWED | Posted: 26 July 2017 doi:10.20944/preprints201707.0076.v1

broaden the global reach of this technology. There is furthermore the prospect of augmenting UV SO_2 imaging with thermal IR camera systems, which are capable for measuring SO_2 (and ash) release by day and night, hence overcoming the limitation of the former spectral region in being reliant upon solar radiation [60]. Finally, there is the potential to widen the number of bands adopted in the cameras to cover absorption by other gas species in order to generate ratio imagery [61]. A clear target here would be bromine monoxide, a species which also has UV absorption features and plays a key role in volcanic plume chemistry [62].

On this theme, we briefly investigated a multi-band approach to imaging gas ratios on Stromboli volcano (during 22-24 July 2015). In this case, conventional UV SO_2 observations were made, in tandem with near-IR (≈ 900nm) imaging, following the technique of Girona et al. [40], who posited that visible pixel brightness is linearly proportional to plume H_2O abundance due to plume scattering. We thereby obtained molar H_2O/SO_2 ratio images, which revealed more water rich compositions for fumarolic discharges vs. crater degassing, as would be expected (Figure 3). We furthermore measured the ratios associated with twenty explosions, and found that H_2O/SO_2 values were reduced by some 50% relative to those during passive degassing, in accord with the ratio reduction during explosions noted in a prior Fourier transform infrared spectroscopy based study on this volcano [63]. These results are very tentative, and at this stage don't consider thermal effects which will change the partitioning of the water between vapour and aerosol phases, hence potentially skewing the H_2O retrievals, where plume temperature changes, e.g., during explosions. Future work, incorporating thermal imagery could be used to constrain this effect, leading to more robust ratio assessments and a broader assessment of the potential utility of this approach in volcanology.

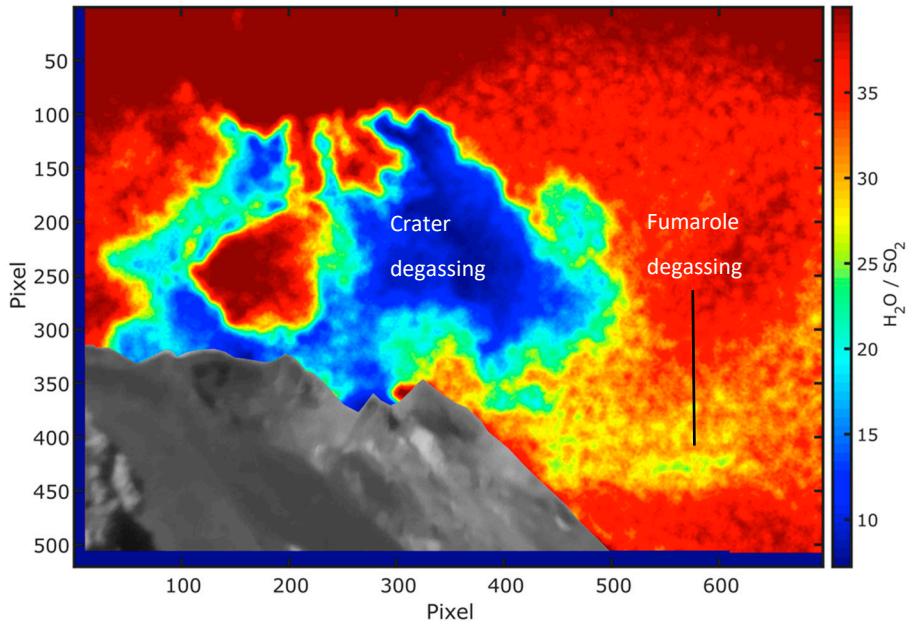

Figure 3. H_2O/SO_2 gas ratio image from Stromboli volcano, with edifice shown in the foreground, based on the methodology described in the main text. The higher (yellow) ratio gas contribution was visually identified as arising from a fumarole on the crater terrace edge, and the lower (blue) ratio component from the gases rising from the craters themselves. Note that these values are arbitrary and uncalibrated at this stage but should still be linearly related to the absolute ratios.

6. Conclusions

Ultraviolet imaging has been applied in volcanology over the last ten years or so, leading to step change improvements in our ability to resolve volcanic gas emissions, both in the temporal and spatial domain, with a user friendly single point measurement configuration. This has led, in particular to capture of rapid gas flux trends associated with explosions, puffing and passive

Preprints (www.preprints.org) | NOT PEER-REVIEWED | Posted: 26 July 2017 doi:10.20944/preprints201707.0076.v1

degassing, in a way that would have been simply impossible, hitherto. A number of groups have now developed UV camera instrumentation [64] and operating software [65], leading to constraints on gas release budgets, and studies into a variety of degassing driven processes, on a wide range of volcanoes, worldwide. In addition, the cameras have the potential to lead to significant scientific breakthroughs by combining the acquired high temporal resolution degassing data with contemporaneous geophysical datasteams, and models for underground gas flows. In recent years we have seen the first steps towards realising these objectives, and evidence of the significant scientific value of these blended approaches. This article looks back at what has been achieved to date, and the considerable promise of UV plume imaging in volcanology going forward.

Acknowledgments: A.J.S.M. acknowledges a Leverhulme Trust Research Fellowship (RF-2016-580), the Rolex Awards for Enterprise and a Google Faculty Research Award (r/136958-11-1). T.D.P. acknowledges the support of a NERC studentship (NE/K500914/1), the University of Sheffield, and ESRC Impact Acceleration funding. T.C.W acknowledges scholarship funding from the University of Sheffield. A.A., M.B., R.D. and G. T. acknowledge support from the European Research Council starting independent research grant (agreement 305377).

Author Contributions: A.J.S.M., T.D.P. and T.C.W wrote the paper. A.J.S.M., T.D.P., T.C.W., G.T., M.B., R.D. and A.A. were involved in designing the experiments, performing the fieldwork and contributing towards the analysis reported on here.

Conflicts of Interest: The authors declare no conflict of interest. The founding sponsors had no role in the design of the study; in the collection, analyses, or interpretation of data; in the writing of the manuscript, and in the decision to publish the results.

References

1. Fischer, T.P.; Chiodini, G. Volcanic, Magmatic and Hydrothermal Gases. In *The Encyclopedia of Volcanoes*, 2nd ed.; Sigurdsson, H., Houghton, B., McNutt, S.R., Rymer, H., Stix, J., Eds.; Academic Press: London, UK, 2015; pp. 779–798.
2. Notsu, K.; Mori, T.; Igarashi, G.; Tohjima, Y.; Wakita, H. Infrared spectral radiometer: A new tool for remote measurement of SO_2 of volcanic gas. *Geochemical Journal*, **1993**, *27*, 361-366.
3. Shinohara, H. A new technique to estimate volcanic gas composition: Plume measurements with a portable multi-sensor system. *J. Volcanol. Geotherm. Res.* **2005**, *143*, 319–333, doi:10.1016/j.jvolgeores.2004.12.004.
4. Santoro, S.; Parracino, S.; Fioriani, L; D'Aleo, R.; Di Ferdinando, E.; Giudice, G.; Maio, G., Nuvoli, M.; Aiuppa, A. Volcanic plume CO_2 measurements at Mount Etna by mobile differential absorption Lidar. *Geosciences* **2017**, *7*, 9, doi:10.3390/geosciences7010009.
5. Stoiber, R.E.; Malinconico, L.L.; Williams, S.N. Use of the correlation spectrometer at volcanoes. In *Forecasting Volcanic Events* (ed. H. Tazieff & J.C. Sabroux), Elsevier, Amsterdam, Netherlands **1983**, pp. 425-444.
6. Sutton, A.J.; Elias, T.; Gerlach, T.M.; Stokes**,** J.B. Implications for eruptive processes as indicated by sulfur dioxide emissions from Kilauea Volcano, Hawaii, 1979-1997. *J. Volcanol. Geotherm. Res.* **2001**, *108*, 283-302, doi: 10.1016/S0377-0273(00)00291-2
7. McGonigle, A.J.S.; Oppenheimer, C.; Galle, B.; Mather, T.A.; Pyle, D.M. Walking traverse and scanning DOAS measurements of volcanic gas emission rates. *Geophys. Res. Lett.* **2002**, *29(20)*, 1985, doi:10.1029/2002GL015827.
8. Galle, B.; Oppenheimer, C.; Geyer, A.; McGonigle, A.J.S.; Edmonds, M.; Horrocks, L.A. A miniaturised UV spectrometer for remote sensing of SO_2 fluxes: a new tool for volcano surveillance. *J. Volcanol. Geotherm. Res.* **2003**, *119*, 241-254, doi: 10.1016/S0377-0273(02)00356-6.
9. Edmonds, M.; Herd, R.A.; Galle, B.; Oppenheimer, C.M. Automated, high time-resolution measurements of SO_2 flux at Soufrière Hills Volcano, Montserrat. *Bull. Volcanol*. **2003**, 65, 578-586, doi: 10.1007/s00445-003-0286-x.
10. McGonigle, A.J.S.; Oppenheimer, C.; Hayes, A.R.; Galle, B.; Edmonds, M.; Caltabiano, T.; Salerno, G. Burton, M.; Mather, T. A. Sulphur dioxide flux measurements at Mount Etna, Vulcano and Stromboli measured with an automated scanning static ultraviolet spectrometer. *J. Geophys. Res.* **2003**, *108(B9)*, 2455, doi:10.1029/2002JB002261

Preprints (www.preprints.org) | NOT PEER-REVIEWED | Posted: 26 July 2017 doi:10.20944/preprints201707.0076.v1

11. Salerno, G.G.; Burton, M.R.; Oppenheimer, C.; Caltabiano, T.; Randazzo, D., Bruno, N.; Longo, V. Three-years of SO_2 flux measurements of Mt. Etna using an automated UV scanner array: Comparison with conventional traverses and uncertainties in flux retrieval. *J Volcanol. Geotherm. Res.* **2009**, 183, 76-83, doi:10.1016/j.jvolgeores.2009.02.013
12. Galle, B.; Johansson, M.; Rivera, C.; Zhang, Y.; Kihlman, M.; Kern, C.; Lehmann, T.; Platt, U.; Arellano, S.; Hidalgo, S. Network for Observation of Volcanic and Atmospheric Change (NOVAC) – A global network of volcanic gas monitoring: Network layout and instrument description. *J. Geophys. Res.* **2010**, 115, D05304, doi: 10.1029/2009JD011823.
13. Mori, T.; Burton, M.R. The SO_2 camera: A simple, fast and cheap method for ground-based imaging of SO_2 in volcanic plumes. *Geophys. Res. Lett.* **2006,** *33*, doi:10.1029/ 2006GL027916.
14. Bluth, G.; Shannon, J.; Watson, I.M.; Prata, A.J.; Realmuto, V. Development of an ultra-violet digital camera for volcanic SO_2 imaging. *J. Volcanol. Geotherm. Res.* **2007**, *161*, 47–56, doi: 10.1016/j.jvolgeores.2006.11.004.
15. Kantzas, E.P.; McGonigle, A.J.S.; Tamburello, G.; Aiuppa, A.; Bryant, R.G. Protocols for UV camera volcanic SO_2 measurements. *J. Volcanol. Geoth. Res.* **2010,** *194*, 55–60, doi:10.1016/j.jvolgeores.2010.05.003.
16. Williams-Jones, G.; Horton, K.A., Elias, T., Garbeil, H., Mouginis-Mark, P.J., Sutton, A.J., Harris, A.J.L. Accurately measuring volcanic plume velocity with multiple UV spectrometers. *Bull. Volc.* **2006,** *68,* 328-332, doi:10.1007/s00445-005-0013-x.
17. McGonigle, A.J.S.; Hilton, D.R.; Fischer, T.P.; Oppenheimer, C. Plume velocity determination for volcanic SO_2 flux measurements. *Geophys. Res. Lett.* **2005**, *32*, L11302. doi: 10.1029/2005GL022470.
18. Peters, N.; Hoffmann, A.; Barnie, T.; Herzog, M.; Oppenheimer C. Use of motion estimation algorithms for improved flux measurements using SO_2 cameras. *J. Volcanol. Geoth. Res.* **2015**, *300*, 58–69, doi:10.1016/j.jvolgeores.2014.08.031.
19. Wilkes, T.C.; McGonigle, A.J.S.; Pering, T.D.; Taggart, A.J.; White, B.S.; Bryant, R.G.; Willmott, J.R. Ultraviolet Imaging with Low Cost Smartphone Sensors: Development and Application of a Raspberry Pi-Based UV Camera. *Sensors* **2016**, *16*, 1649, doi:10.3390/s16101649.
20. Wilkes, T.C., Pering, T.D., McGonigle, A.J.S., Tamburello, G., Willmott, J.R. A low cost smartphone sensor-based UV camera for volcanic SO_2 emission measurements, *Rem. Sens.*, **2017**, *9*, 27, doi:10.3390/rs9010027.
21. Holland, A.S.P.; Watson, I.M.; Phillips, J.C.; Caricchi, L.; Dalton, M.P. Degassing processes during lava dome growth: insights from Santiaguito Lava Dome, Guatemala. *J. Volcanol. Geotherm. Res.* **2011**, *202*, 153–166, doi:10.1016/j.jvolgeores.2011.02.004.
22. Campion, R.A.; Delgado-Granados, H.; Mori, T. Image-based correction of the light dilution effect for SO_2 camera measurements, *J. Volcanol. Geotherm. Res.* **2015**, *300*, 48-57, doi:10.1016/j.jvolgeores.2015.01.004.
23. Kern, C.; Werner, C.; Elias, T.; Sutton, A.J.; Lübcke, P. Applying UV cameras for SO_2 detection to distant or optically thick volcanic plumes. *J. Volcanol. Geotherm. Res.* **2013**, *262*, 80–89, doi:10.1016/j.jvolgeores.2013.06.009.
24. Lübcke, P.; Bobrowski, N.; Illing, S.; Kern, C.; Alvarez Nieves, J.M.; Vogel, L.; Zielcke, J.; Delgado Granados, H.; Platt, U. On the absolute calibration of SO_2 cameras. *Atmos. Meas. Tech.* **2013**, *6*, 677–696. doi:10.5194/amt-6-677-2013.
25. Kern, C.; Kick, F.; Lübcke, P.; Vogel, L.; Wöhrbach, M.; Platt, U. Theoretical description of functionality, applications, and limitations of SO_2 cameras for the remote sensing of volcanic plumes. *Atmos. Meas. Tech.* **2010**, 3, 733-749, doi:10.5194/amt-3-733-2010.
26. Kuhn, J.; Bobrowski, N.; Lübcke, P.; Vogel, L.; Platt, U. A Fabry-Perot interferometer-based camera for two-dimensional mapping of SO_2 distributions. *Atmos. Meas. Tech.* **2014**, 7, 3705-3715, doi:10.5194/amt-7-3705-2014.
27. Platt, U.; Lübcke, P.; Kuhn, J.; Bobrowski, N.; Prata, F.; Burton, M.; Kern, C. Quantitative imaging of volcanic plumes – Results, needs, and future trends. *J. Volcanol. Geotherm. Res.* **2015**, *300*, 7-21, doi:10.1016/j.jvolgeores.2014.10.006.
28. Campion, R.; Martinez-Cruz, M.; Lecocq, T.; Caudron, C.; Pacheco, J.; Pinardi, G.; Hermans, C.; Carn, S.; Bernard, A. Space- and ground-based measurements of sulphur dioxide emissions from Turrialba Volcano (Costa Rica). *Bull. Volcanol.* **2012**, *74*, 1757–1770, doi:10.1007/s00445-012-0631-z.

Preprints (www.preprints.org) | NOT PEER-REVIEWED | Posted: 26 July 2017 doi:10.20944/preprints201707.0076.v1

29. Stebel, K.; Amigo, A.; Thomas, H.E.; Prata, A.J. First estimates of fumarolic SO_2 fluxes from Putana volcano, Chile, using an ultraviolet imaging camera. *J. Volcanol. Geotherm. Res.* **2015**, *300*, 112–120, doi:10.1016/j.jvolgeores.2014.12.021.
30. Kern, C.; Sutton, J.; Elias, T.; Lee, L.; Kamibayashi, K.; Antolik, L. An automated SO_2 camera system for continuous, real-time monitoring of gas emissions from Kīlauea Volcano's summit Overlook Crater. *J. Volcanol. Geotherm. Res.* **2015**, *300*, 81–94, doi:10.1016/j.jvolgeores.2014.12.004.
31. D'Aleo, R.; Bitetto, M.; Delle Donne, D.; Tamburello, G.; Battaglia, A.; Coltelli, M.; Patanè, D.; Prestifilippo, M.; Sciotto, M.; Aiuppa, A. Spatially resolved SO_2 flux emissions from Mt Etna. *Geophys. Res. Lett.* **2016**, *43*, 7511–7519, doi:10.1002/2016GL069938.
32. Delle Donne, D.; Ripepe, M.; Lacanna, G.; Tamburello, G.; Bitetto, M.; Aiuppa, A. Gas mass derived by infrasound and UV cameras: Implications for mass flow rate. *J. Volcanol. Geotherm. Res.* **2016**, *325*, 169-178, doi:10.1016/j.jvolgeores.2016.06.015.
33. Pering, T.D.; McGonigle, A.J.S.; James, M.R.; Tamburello, G.; Aiuppa, A.; Delle Donne, D.; Ripepe, M. Conduit dynamics and post explosion degassing on Stromboli: a combined UV camera and numerical modelling treatment. *Geophys. Res. Lett.* **2016**, *43*, 5009-5016, doi: 10.1002/2016GL069001.
34. Burton, M.R.; Salerno, G.G.; D'Auria, L.; Caltabiano, T.; Murè, F.; Maugeri, R. SO_2 flux monitoring at Stromboli with the new permanent INGV SO_2 camera system: A comparison with the FLAME network and seismological data. *J. Volcanol. Geotherm. Res.* **2015**, *300*, 95–102. doi:10.1016/j.jvolgeores.2015.02.006.
35. Aiuppa, A.; Giudice, G., Gurrieri, S., Liuzzo, M., Burton, M., Caltabiano, T., McGonigle, A.J.S., Salerno, G., Shinohara, H., Valenza, M. Total volatile flux from Mount Etna. *Geophys. Res. Lett.* **2008,** *35* doi:10.1029/2008GL035871.
36. Tamburello, G.; Kantzas, E.P.; McGonigle, A.J.S.; Aiuppa, A.; Giudice G. UV camera measurements of fumarole field degassing (La Fossa crater, Vulcano Island). *J. Volcanol. Geotherm. Res.* **2011**, *199*, 47-52, doi:10.1016/j.jvolgeores.2010.10.004.
37. Tamburello, G.; Aiuppa, A.; McGonigle, A.J.S.; Allard, P.; Cannata, A.; Giudice, G.; Kantzas, E.P.; Pering, T.D. Periodic volcanic degassing behavior: the Mount Etna example. *Geophys. Res. Lett.* **2013**, *40*, 4818–4822, doi:10.1016/j.epsl.2012.09.050.
38. McGonigle, A.J.S.; Aiuppa, A.; Ripepe, M.; Kantzas, E.P.; Tamburello, G. Spectroscopic capture of 1 Hz volcanic SO_2 fluxes and integration with volcano geophysical data. *Geophys. Res. Lett.* **2009**, *36*, L21309, doi:10.1029/2009GL040494.
39. Boichu, M.; Oppenheimer, C., Tsanev, V., Kyle, P.R. High temporal resolution SO_2 flux measurements at Erebus volcano, Antarctica. *J. Volcanol. Geotherm. Res.* **2010,** *190,* 325-336, doi:10.1016/j.volgeores.2009.11.020.
40. Girona, T.; Costa, F., Taisne, B., Aggangan, B., Ildefonso, S. Fractal degassing from Erebus and Mayon volcanoes revealed by a new method to monitor H_2O emission cycles. *J. Geophys. Res-Solid.* **2015,** *120,* 2,988-3,002, doi:10.1002/2014JB011797.
41. Pering, T.D., McGonigle, A.J.S., Tamburello, G., Aiuppa, A., Bitetto, M., Rubino, C., Wilkes T.C. A novel and inexpensive method for measuring volcanic plume water fluxes at high temporal resolution, *Rem Sens.*, **2017**, 9, 146, doi:10.3390/rs9020146.
42. Pering, T.D.; Tamburello, G.; McGonigle, A.J.S.; Aiuppa, A.; Cannata, A.; Giudice, G.; Patanè, D. High time resolution fluctuations in volcanic carbon dioxide degassing from Mount Etna. *J. Volcanol. Geotherm. Res.* **2014**, *270*, 115–121, doi:10.1016/j.jvolgeores.2013.11.014.
43. Moussallam, Y.; Bani, P.; Curtis, A.; Barnie, T.; Moussallam, M.; Peters, N.; Schipper, C.I.; Aiuppa, A.; Giudice, G.; Amigo, Á.; Velasquez, G.; Cardona, C. Sustaining persistent lava lakes: Observations from high-resolution gas measurements at Villarrica volcano, Chile. *Earth Planet. Sci. Lett.* **2016**, *454*, 237–247, doi:10.1016/j.epsl.2016.09.012.
44. Nadeau, P.A.; Werner, C.; Waite, G.P.; Carn, S.A.; Brewer, I.D.; Elias, T.; Sutton, A.J.; Kern, C. Using SO_2 camera imagery to examine degassing and gas accumulation at Kīlauea volcano. *J. Volcanol. Geotherm. Res.* **2015**, *300*, 103-111, doi:10.1016/j.jvolgeores.2014.12.005.
45. Fischer, T.P.; Roggensack, K.; Kyle, P.R. Open and almost shut case for explosive eruptions: Vent processes determined by SO_2 emission rates at Karymsky volcano, Kamchatka. *Geology* **2002**, *30*, 1059-1062, doi:10.1130/0091-7613(2002)030<1059:OAASCF>2.0.CO;2.

Preprints (www.preprints.org) | NOT PEER-REVIEWED | Posted: 26 July 2017 doi:10.20944/preprints201707.0076.v1

46. Yamamoto, H.; Watson, I.M.; Phillips, J.C.; Bluth, G.J. Rise dynamics and relative ash distribution in vulcanian eruption plumes at Santiaguito Volcano, Guatemala, revealed using an ultraviolet imaging camera. *Geophys. Res. Lett.* **2008**, *35*, L08314, doi:10.1029/2007GL032008.
47. Tamburello, G.; Aiuppa, A.; Kantzas, E.P.; McGonigle, A.J.S.; Ripepe, M. Passive vs. active degassing modes at an open-vent volcano (Stromboli, Italy). *Earth Planet. Sci. Lett.* **2012**, *359*, 106–116.
48. Mori T.; Burton M. Quantification of the gas mass emitted during single explosions on Stromboli with the SO_2 imaging camera. *J. Volcanol. Geotherm. Res.* **2009**, *188*, 395–400, doi:10.1016/j.jvolgeores.2009.10.005.
49. Pering, T.D.; Tamburello, G.; McGonigle, A.J.S.; Aiuppa, A.; James, M.R.; Lane, S.J.; Sciotto, M.; Cannata, A.; Patanè, D. Dynamics of mild strombolian activity on Mt. Etna. *J. Volcanol. Geotherm. Res.* **2015**, *300*, 103–111, doi: 10.1016/j.jvolgeores.2014.12.013.
50. Smekens, J-F.; Clarke, A.B.; Burton, M.R.; Harijoko, A.; Wibowo, H. SO_2 emissions at Semeru volcano, Indonesia: characterization and quantification of persistent periodic explosive activity. *J. Volcanol. Geotherm. Res.* **2015**, *300*, 121-128, doi:10.1016/j.jvolgeores.2015.01.006.
51. Kazahaya, R.; Mori, T.; Takeo, M.; Ohminato, T.; Urabe, T.; Maeda, Y. Relation between single very-long-period pulses and volcanic gas emissions at Mt. Asama, Japan. *Geophys. Res. Lett.* **2011**, *38*, L11307, doi:10.1029/2011GL047555.
52. Waite, G.P.; Nadeau, P.A.; Lyons, J.J. Variability in eruption style and associated very long period events at Fuego volcano, Guatemala. *J. Geophys. Res. Sol. Ea.* **2013**, *118*, 1526-1533, doi: 10.1002/jgrb.50075.
53. James, M.R.; Lane, S.J.; Wilson, L.; Corder, S.B. Degassing at low magma-viscosity volcanoes: Quantifying the transition between passive bubble-burst and Strombolian eruption. *J. Volcanol. Geotherm. Res.* **2009**, *180*, 81-88, doi:10.1016/j.jvolgeores.2008.09.002.
54. Gaudin, D.; Taddeucci, J.; Scarlato, P.; Harris, A.; Bombrun, M.; Del Bello, E.; Ricci, T.; Characteristics of puffing activity revealed by ground-based, thermal infrared imaging: the example of Stromboli volcano (Italy). *Bull Volcanol.* **2007**, *79*, 24, doi:10.1007/s00445-017-1108-x.
55. Nadeau, P.A.; Palma, J.L.; Waite, G.P. Linking volcanic tremor, degassing, and eruption dynamics with SO_2 imaging. *Geophys. Res. Lett.* **2011**, *38*, L013404, doi:10.1029/2010GL045820.
56. Pering, T.D.; Tamburello, G., McGonigle, A.J.S., Hanna, E., Aiuppa, A. Correlation of oscillatory behaviour in Matlab using wavelets. *Comput. Geosci.* **2014,** *70,* 206-212, doi:10.1016/j.cageo.2014.06.006.
57. Dalton, M.P.; Waite, G.P.; Watson, I.M.; Nadeau, P.A. Multiparameter quantification of gas release during weak Strombolian eruptions at Pacaya Volcano, Guatemala. *Geophys. Res. Lett.* **2010**, *37*, L09303, doi:10.1029/2010GL042617.
58. Fischer, T.P.; Morrissey, M.M.; Calvache M.L.V.; Gómez, D.M.; Torres, R.C.; Stix, J.; Williams. S.N.; Correlations between SO_2 flux and long-period seismicity at Galeras volcano. *Nature* **1994**, *368*, 135-137.
59. Lopez, T.; Thomas, H.; Prata, A.J.; Amigo, A.; Fee, D.; Moriano, D.; Volcanic Plume Characteristics Determined Using an Infrared Imaging Camera. *J. Volcanol. Geotherm. Res.* **2015**, *300*, 148–166, doi:10.1016/j.jvolgeores.2014.12.009.
60. McCormick Kilbride, B.; Edmonds, M.; Biggs, J.; Observing eruptions of gas-rich compressible magmas from space. *Nat. Commun.* **2016**, *7*, 13744, doi:10.1038/ncomms13744.
61. Burton, M.R.; Prata, F.; Platt, U.; Volcanological applications of SO_2 cameras. *J. Volcanol. Geotherm. Res.* **2015**, *300*, 2–6, doi: 10.1016/j. jvolgeores.2014.09.008.
62. von Glasow, R.: Atmospheric chemistry in volcanic plumes, *P. Natl. Acad. Sci. USA* **2010**, *107*, 6594–6599, doi:10.1073/pnas.0913164107.
63. Burton, M.; Allard, P.; Muré, La Spina. A.; Magmatic gas composition reveals the source depth of slug-driven strombolian explosive activity. *Science* **2007**, *317*, 227, doi:10.1126/science.1141900.
64. Kern, C.; Lübcke, P.; Bobrowski, N.; Campion, R.; Mori, T.; Smekens, J.-F.; Stebel, K.; Tamburello, G.; Burton, M.R.; Platt, U.; Prata, F.; Intercomparison of SO_2 camera systems for imaging volcanic gas plumes. *J. Volcanol. Geotherm. Res.* **2015**, *300*, 22–36, doi: 10.1016/j. jvolgeores.2014.08.026.
65. Tamburello, G.; Kantzas, E.P.; McGonigle, A.J.S.; Aiuppa, A.; Vulcamera: A program for measuring volcanic SO_2 using UV cameras. *Ann. Geophys.* **2011**, *54*, 219–221, doi:10.4401/ag-5181.